BioChip J. (2017) 11(2): 153-163
DOI 10.1007/s13206-017-1304-y

Original Article

Flexible and Implantable Capacitive Microelectrode for Bio-potential Acquisition

Seung Min Lee[1,†], Hang Jin Byeon[2,†], Bong Hoon Kim[3], Jungyup Lee[3], Ji Yoon Jeong[3], Joong Hoon Lee[4], Jin-Hee Moon[5], Cheolsoo Park[6], Hyuk Choi[7,*], Sang-Hoon Lee[4] & Kwang-Ho Lee[8,*]

Received: 15 February, 2017 / Accepted: 23 March, 2017 / Published online: 02 June, 2017

Abstract Electrodes should be adhered onto the body steadily under motion, and implanted stably into the tissue without any damages while maintaining conformal contact. Although most electrodes are fabricated with biocompatible materials, they should be shielded from tissues to prevent mechanical delamination from the device itself and to avoid adverse effects such as irritation, allergic reactions, or inflammation. Herein, we demonstrate a simple process for the development of a flexible and implantable capacitive electrode based on a minimal incision accessible design with polyimide (PI) and Gold/Titanium (Au/Ti) layers and completely encapsulated in a polydimethylsiloxane (PDMS) substrate. Electrodes of three different sizes (recording site diameters of 1.8 mm, 2.8 mm, and 3.8 mm, respectively) were fabricated and examined in this work. Electrocardiography (ECG) was recorded in the dorsal area of the rat for 4 weeks for biological signal checkup. We obtained stable and robust ECG signals owing to the intrinsic property of capacitive coupling, with almost no leakage current compared to the direct contact electrode for the applied current over the range of 0 to 10 mA. These results indicate that our electrode can be used to detect bio-signals effectively in the long term, and can play a role in electroceuticals in the near future.

Keywords: Electrode: Polydimethylsiloxane (PDMS), Gold/Titanium (Au/Ti), Electrocardiography (ECG), Capacitive Coupling, Bio-potential

[1]School of Electrical Engineering, College of Creative Engineering, Kookmin University, Seoul 02707, Republic of Korea
[2]Sensor Solution Lab, Material & Production Research Institute, LG Electronics, Woomyun R&D Campus, Seoul 06755, Republic of Korea
[3]Department of Materials Science and Engineering, University of Illinois at Urbana-Champaign, Urbana, Illinois 61801, USA
[4]Department of Biomedical Engineering, College of Health Science, Korea University, Seoul 02841, Republic of Korea
[5]Department of Research & Development of Medical Device Development Center in Osong Medical Innovation Foundation, Cheongju 28160, Republic of Korea
[6]Department of Computer Engineering, Kwangwoon University, Seoul 01897, Republic of Korea
[7]Department of Medical Science, Graduate School of Medicine, Korea University, Seoul 02841, Republic of Korea
[8]Department of Advanced Material Science and Engineering, College of Engineering, Kangwon National University, Chuncheon 25561, Republic of Korea
[†]These authors contributed equally to this work.
*Correspondence and requests for materials should be addressed to H. Choi (✉hyuk76@korea.ac.kr) and K-H. Lee (✉khmhlee@kangwon.ac.kr)

Introduction

Continuous monitoring of bio-signals is required to detect intermittent or infrequent diseases such as syncope, arrhythmia, epilepsy etc[1-4]. Furthermore, reliable and high quality electrodes are paramount to acquire high fidelity bio-signals. Currently, wet electrodes such as Ag/AgCl electrodes are widely employed to measure bio-signals from the surface of the body by mounting and fixing them on the skin. However, the periodic replacement of electrode and the occurrence of disturbances restrict physical activities including sleep, shower, and exercise. A wet electrode is often utilized for the electrical contact between the electrode and skin. However, it dries out over time and results in distorted bio-signals. A stronger adhesion layer in this electrode is associated with skin irritation and rash. Hence, Ag/AgCl electrode is not appropriate for con-

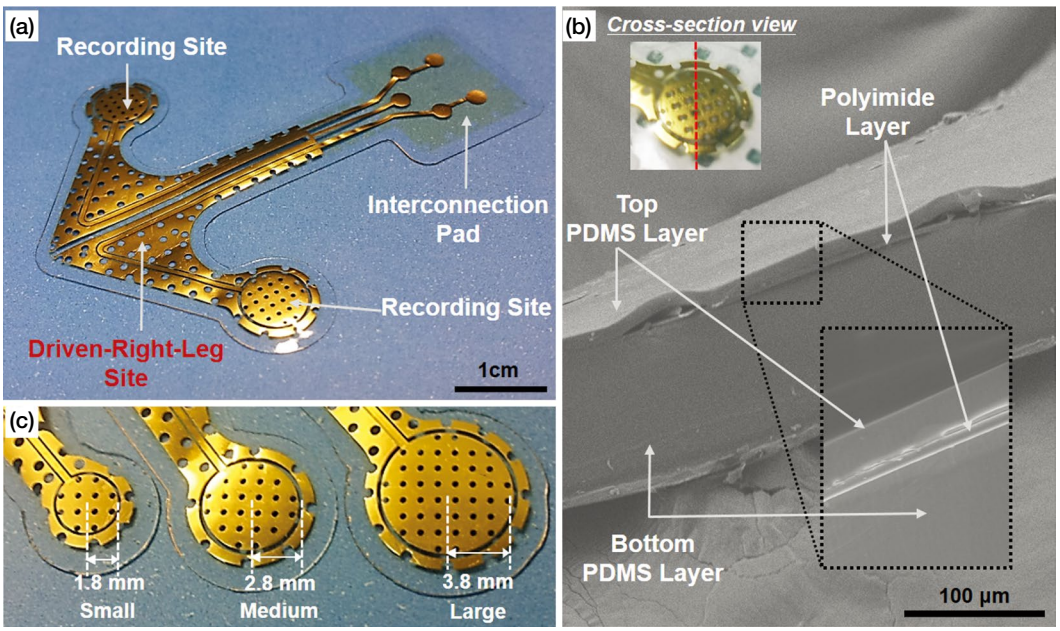

Figure 1. (a) View of developed electrode, (b) Cross sectional SEM image of electrode, and (c) 3 different electrodes with different diameter sizes: Small (*r*: 1.8 mm), Medium (*r*: 2.8 mm), Large (*r*: 3.8 mm).

tinuous monitoring. Accordingly, skin-like electrodes with bio-compatible substrates have been developed to overcome these problems[5-8]. These electrodes exhibit mechanical properties of the skin and consequently, result in a conformal contact with the skin. Although these electrodes can reduce disturbances, stable and durable bio-signal measurement has been challenging. These limitations have led to the development of implantable electrodes using a variety of materials including silicon, ceramic, and platinum[9-14]. Although these electrodes have recorded relatively stable bio-signals, they are generally inflexible and unyielding. Moreover, the metal delaminates under certain circumstances and over a long period[15-17]. Besides, electrical safety, biocompatibility, and especially interaction between the metal and the surrounding tissue are major challenges[18]. These risks can be avoided by preventing direct contact between the metal layers and the tissue. In this perspective, capacitive recording is an alternative sensing technique for continuous monitoring. Capacitive measurement senses through the insulating layer by coupling the target area and electrode as a capacitive pathway with no direct charge exchange or flow; hence, it eliminates the problem of current leakage[6,19].

In this paper, we present a flexible and implantable capacitive polydimethylsiloxane (PDMS)-encapsulated electrode for the measurement of physiological signals. Further, the tissues are in contact with the surface of PDMS, which is a highly bio-compatible material with chemical and mechanical stability[20-23]. This electrode overcomes the aforementioned problems associated with direct metal-tissue contacting electrodes. Moreover, the encapsulated PDMS prevents delamination of the metal layer by holding it tightly. Owing to the low electrical conductivity of PDMS, this electrode improves the electrical safety by dramatically minimizing the leakage current as compared to the direct contact electrodes[24-26]. This electrode was implanted under the epidermis of a rat, and subsequently ECG signal was measured. For 4 weeks, the electrical characteristics and biocompatibility of the developed electrode were evaluated.

Results and Discussion

Fabrication of Electrode

The electrode was successfully fabricated as shown in Figure 1(a). The driven-right leg (DRL) site covered most of the remaining area of the first PI layer since a large DRL site can effectively lead to common voltage reduction[27,28]. The longitudinal length of the fabricated electrode was 5 cm. The cross-sectional scanning electron microscopy (SEM) image of the electrode is shown in Figure 1(b). Furthermore, the total thickness of the electrode was approximately 125 μm and the top PDMS layer has a thickness of 13 μm. The electrodes of three different diameters (small (*r*: 1.8 mm), medium

(*r*: 2.8 mm), and large (*r*: 3.8 mm)) of the recording site are shown in Figure 1(c).

Electrode Impedance and Curve Fitting Results

The electrodes were immersed and kept in the phosphate-buffered saline (PBS) at 36°C for 28 days. The impedance of electrode was measured on days 0, 3, 7, 14, 21, and 28. Since the electrode was fully encapsulated in PDMS, it exhibits relatively high impedance with a large standard error as compared to the direct contact electrode over the frequency range tested. The impedance decreased when the frequency increased owing to capacitive coupling effects as shown in Figure 2. After the electrode was immersed in PBS, the impedance was the highest on day 0, and the impedance kept decreasing as the days passed. Particularly, the impedance dropped dramatically on day 3. Based on the interface model, R_{PDMS} and C_{PDMS} were calculated using a curve-fitting method. Table 1 shows the calculated R_{PDMS} and C_{PDMS} values and Pearson's correlations were calculated from the curve fits. After the immersion of electrode, R_{PDMS} (Z_R) and C_{PDMS} (Z_C) impedance values decreased as the PBS permeated into the PDMS layer. After 28 days, Z_R decreased to 7.0×10^8 Ω and Z_C decreased to 5.7×10^5 Ω at 100 Hz, which is the frequency of the rat QRS waves. Most of the signals were delivered by the capacitive coupling effect since Z_C was only 0.081% of the Z_R.

Noise and Leakage Current Characteristics

The Figure 3(a) shows the noise characteristics of both 'as-prepared' electrode and the electrode immersed in PBS for 28 days. The PBS immersed electrode had a reduced power spectrum density (PSD) as compared to 'as-prepared' electrode. Therefore, as time passes by, the common noise level is reduced and a higher signal quality level is induced. The result of the leakage cur-

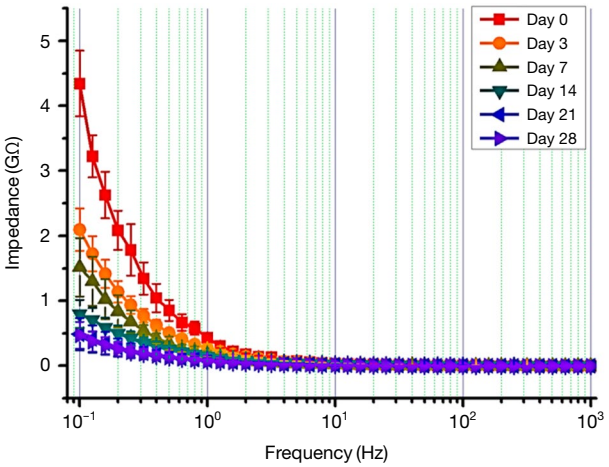

Figure 2. Impedance analysis and electrode measurements collected *in vitro*, in a PBS solution. Five electrodes (large size) were immersed in PBS maintained at 36°C, and sensing measurements were collected over 28 days. The values were simulated using the Trust-Region algorithm.

Table 1. Simulation of the electrode performance during immersion in PBS.

	R_{PDMS} (Ω)	C_{PDMS} (F)	Z_C (Ω) at 100 Hz	Adj. R^2
Day 0	1.1×10^{10}	3.8×10^{-10}	4.2×10^6	0.9985
3	3.5×10^9	6.4×10^{-10}	2.5×10^6	0.9746
7	2.8×10^9	9.0×10^{-10}	1.7×10^6	0.9843
14	1.0×10^9	1.4×10^{-9}	1.1×10^6	0.9923
21	7.1×10^8	2.5×10^{-9}	6.4×10^5	0.9311
28	7.0×10^8	2.8×10^{-9}	5.7×10^5	0.9544

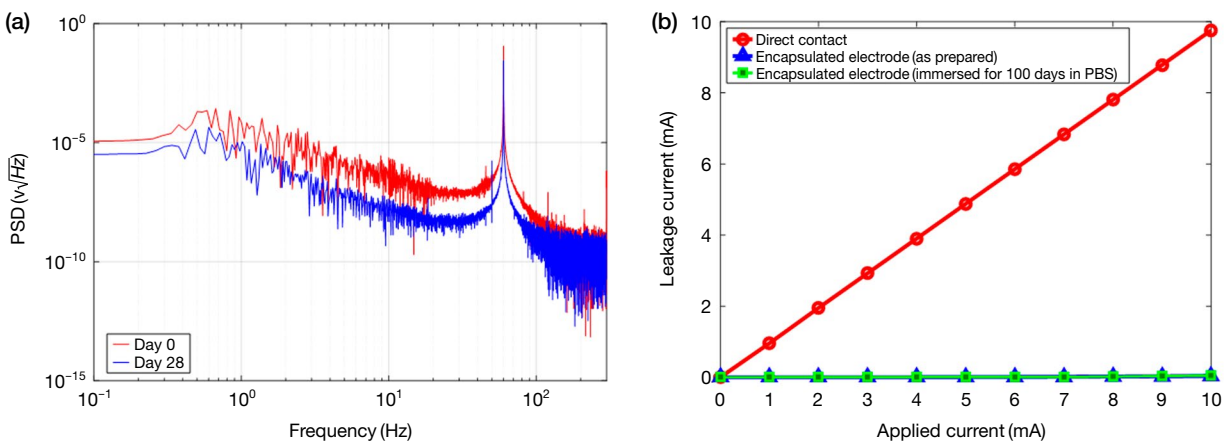

Figure 3. (a) PSD of the noise in a signal acquired with 'as prepared' and 28 days after immersion in PBS electrodes. (b) Leakage current measurements obtained using three different electrodes: a direct-contact electrode, an as-prepared encapsulated (capacitive) electrode, and an encapsulated (capacitive) electrode immersed for 100 days in PBS.

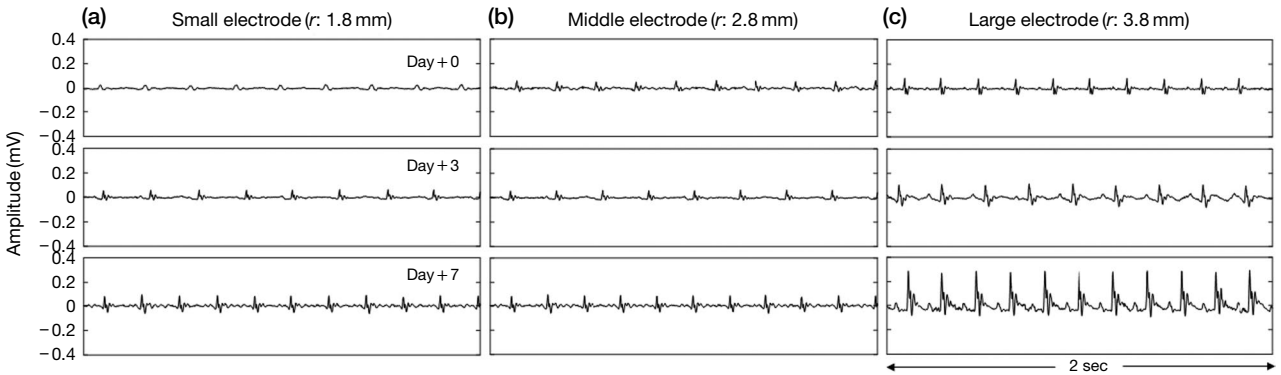

Figure 4. ECG signals acquired on days 0, 3, and 7 after implantation, using (a) a small electrode, (b) a medium electrode, and (c) a large electrode.

rent of both the aforementioned electrodes is shown in Figure 3(b). The result indicates that both electrodes had extremely small leakage current as compared to the direct contact electrode for the applied current over the range of 0 to 10 mA. More than 99% of the applied current was blocked in the case of the non-contact electrode and the PBS-immersed and 'as-prepared' electrodes were not distinguishable.

ECG Acquisition

In Figure 4(a-c), the ECG waveforms acquired using three different sizes of electrode, small (*r*: 1.8 mm), medium (*r*: 2.8 mm), and large (*r*: 3.8 mm), are shown. With a larger electrode, the ECG signal was stronger and clearer on every acquisition day. On day 0, with a small electrode, the ECG signal was distorted, attenuated, and compressed. Moreover, the signal was less distorted and the amplitude was larger as the electrode size increased. The amplitude of the signal increased after the implantation, as days passed, for all sizes of the electrodes. The signals became the strongest after day 7 and remained so for 4 weeks as shown in Figure 5.

Biocompatibility Test

Some tissue samples were collected from the area around the implanted electrode to conduct histological analysis using H&E staining. Figure 6(a) shows the site where the electrode was implanted for 4 weeks. No tissue infection or inflammation was observed by visual inspection. Figure 6(b) shows the result of the H&E staining, and there was no inflammation or infection. When the encapsulated electrode was implanted over 4 weeks, it remained intact without any damages as shown in Figure 6(c). However, when the PDMS encapsulation was not applied, the metal layer was delaminated from the PI layer (Figure 6(d)).

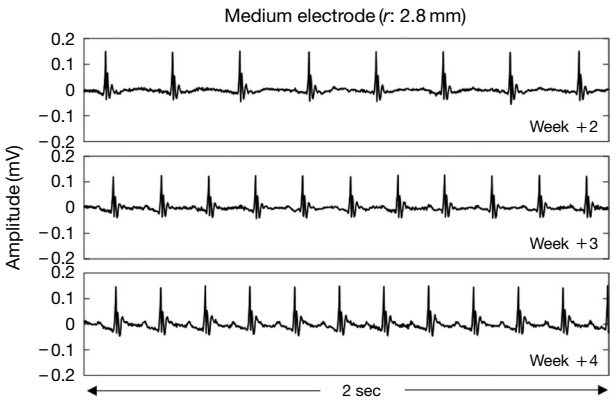

Figure 5. ECG signals acquired 2, 3, and 4 weeks after implantation from medium sized electrode (*r*: 2.8 mm).

We proposed a method to measure the physiological signals by using fully PDMS-encapsulated capacitive electrodes. The electrode showed good adhesion properties enough to be implanted on the dorsal area of a rat without additional sutures; furthermore, it was non-toxic, non-flammable, even flexible on an irregular surface and highly biocompatible. It is suitable for developing medical and implantable devices with PDMS[5,10,29,30]. The developed flexible electrode performed non-contact signal measurement, via capacitive-coupling; further, PDMS acted as an insulating layer that prevented the direct contact between the tissues and the metal layer. Furthermore, the encapsulated PDMS protected the 100 nm thick Au metal patterns on the PI layers from physical and chemical damage. Without the PDMS layer, Au metal patterns were delaminated when implanted on the back of rats for 4 weeks owing to chemical reactions, shear stress with fluids, and friction stress between the tissues

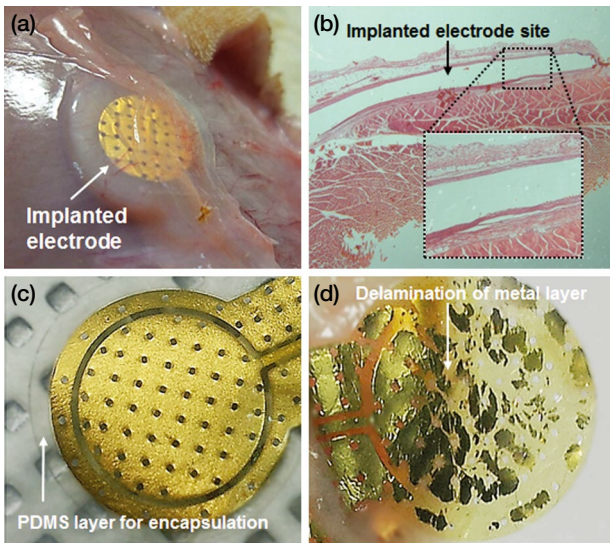

Figure 6. (a) Photograph showing the implantation site used in the biocompatibility test, (b) Images of the H&E stained tissues collected from the implant area, (c) PDMS-encapsulated and (d) non-encapsulation electrodes, retrieved 4 weeks after subcutaneous *in vivo* implantation.

and the metal layer (Figure 6(a)). The weakness of the adhesive bond between the PI and Au reported in a previous study also supports this phenomenon[31]. In this study, the metal patterns encapsulated by PDMS were perfectly maintained (Figure 6(b)) as PDMS held patterns tightly and acted as a stress absorber. In this view, the place where the electrode is sutured and the folding event may be critical for aging. As the electrode was implanted in the back side, it is expected to be less affected by mechanical fatigue and/or flexibility. Furthermore, owing to the intrinsic property of capacitive coupling, the developed electrode was free from electrical damages. As shown in Figure 3(b), since the metal layer was encapsulated by PDMS, the leakage current was not detected. However, it was proportional to the applied voltage for the electrode without PDMS encapsulation. Since capacitive-coupling measures the displacement current, the signal quality was sensitive to the electrode area, distance between the signal source and electrode, and dielectric constant of the insulation layer[32,33]. In this study, the larger electrode showed better signal quality as shown in Figure 4. Furthermore, the ECG signal was found to be sensitive to the number of days elapsed after implantation. The reason of this behavior is explained by increased dielectric constant owing to the uptake of bio-fluid resulting lowered impedance[10,30]. According to the PBS test, the impedance decreases as the PBS solution soaks the PDMS layer resulting in lowered impedance. The result from impedance analyzer, C_{PDMS} increased which resulted in lowered Z_C, as shown in Table 1 and Figure 5. At the same time it also decreased R_{PDMS} so the impedance of the PDMS is affected by in capacitive and conductive way. However, the impedance caused by conductive path is much higher than that of capacitive path so signal is dominantly measured in capacitive path, and R_{PDMS} is high enough to prevent the leakage current even after the PBS buffer had fully diffused into the PDMS layer, as the impedance from the capacitance was much lower than the impedance of the resistance at 100 Hz over the period. In this view, if the electrode was merged in the PBS solution before the use, clear ECG signal could be captured at the beginning of measurement, so there is no need to wait until signal becomes clean. As the interface was established mostly by capacitive way, size of recording site is a critical factor for the signal quality. Once the size of recording site increased, capacitance increased which reduces the impedance. Therefore larger recording site induces higher signal quality. However, at the same time, the recording site might affect the ECG waveform as it also smooths the signal[32]. Therefore optimal size should be determined by considering the size of subject. Though the thickness of insulating layer is also important factor for signal quality as well for the capacitive measurements, too thin electrodes are easily folded so large area of the skin should be opened for implant procedure. In our experience, the developed PDMS encapsulated electrode is reasonably well recovered to its original shape even though it was inserted through incision of only approximately 2 cm. These types of electrode reveal the tradeoffs between high selectivity and simplicity of the fabrication process. Accordingly, other groups have tried to reduce the impedance of the electrode by fabricating a carbon nanotube/PDMS or a nickel/PDMS composite; however, these methods require skilled manual labor[34]. Our electrode fabrication process is straightforward in comparison with the abovementioned methods, and our results exhibit a good performance for the recording of bio-signals. Furthermore, in the visual inspection after 4 weeks, the fibrous tissue wrapped around and tightly fixated the electrode, which was found to be positioned stably in the tissue, without incurring any damage. The stability resulting from the tissues wrapped around the electrode ensured reliability and showed conformal contact. Previous studies have emphasized contact status between an electrode and tissue in case capacitive-coupling used[6,7,19,32]. This conformal fixation permits the electrode to adjust mechanically during the movement. Since the electrode was inserted easily in the subcutaneous region owing to our unique

design, natural pressure may be applied at the electrode site to enhance the contact between the electrode and tissue and hence, the encapsulated electrode could adapt to the curvature of the body. By means of the biocompatibility, electrical safety, and perfect conformal contact of the developed electrode demonstrated in this paper, this approach may potentially be used as a diagnosis tool in subjects without body movement restrictions.

Conclusion

In summary, the developed fully PDMS-encapsulated electrode using the capacitive sensing approach can successfully acquire ECG signals under *in vivo* conditions. The electrode ensured biocompatibility and protected the metal pattern from physical and chemical damage in dynamic and fluidic environments. A tightly fixated and flexible electrode enhanced contact status on the irregular surface. Further, with enhanced electrical status via the body fluid, it resulted in enhanced ECG signal qualities. The proposed electrode can be utilized to monitor several biological signals without any risks that may result from direct metal contact with the tissue.

Materials and Methods

Electrode Design

In order to acquire ECG signals from a rat, the structure of the electrode was designed as an arrow shape for convenient insertion into the subcutaneous region of rat as shown in Figure 7(a). This arrow-shaped electrode could minimize the incision area needed for the insertion of the electrode. Two recording sites with equal surface areas were symmetrically located on the left and right sides for capturing ECG signals, and the rest of the area was covered with a DRL electrode in which the circuit is added to biological signal amplifiers to reduce common-mode interference. The DRL area is used for active noise cancellation. Further, shielding lines patterns are deposited above the recording interconnection lines to prevent external noise

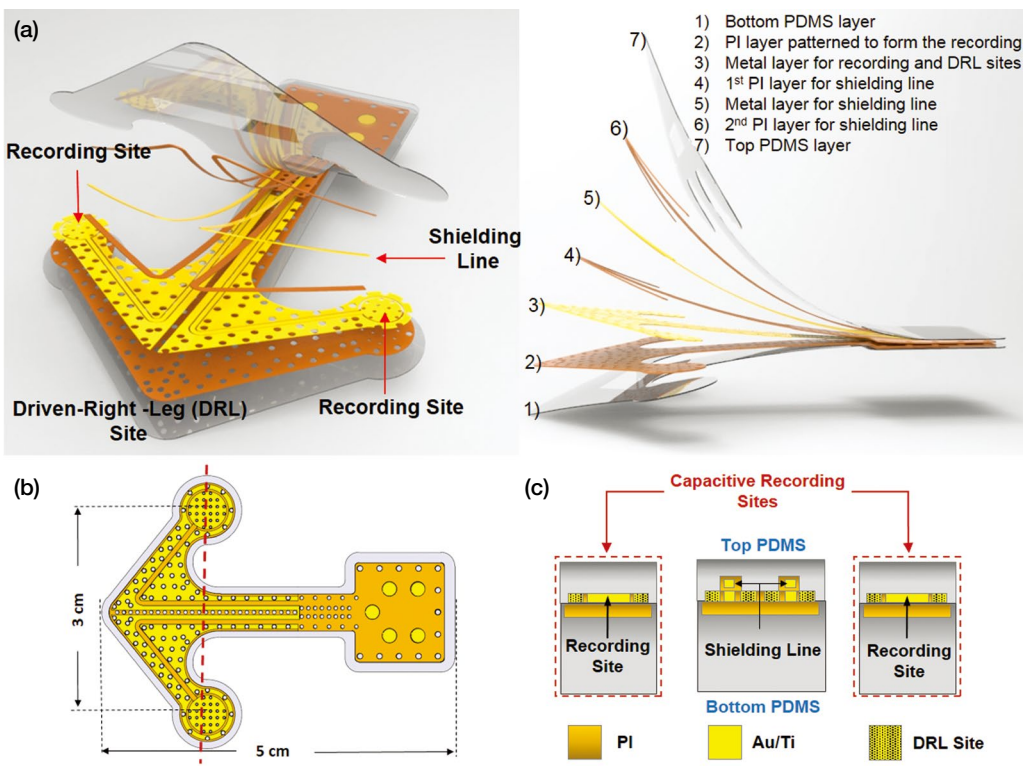

Figure 7. Schematic illustration of the electrode structure. (a) Schematic diagram of each electrode layer; 1) Bottom PDMS layer, 2) PI layer patterned to form the recording, 3) Metal layer for recording DRL sites, 4) 1st PI layer for shielding line, 5) Metal layer for shielding line, 6) 2nd PI layer for shielding line, and 7) Top PDMS layer, (b) Top view layout of the electrode, and (c) Schematic illustration of cross-sectional view of the electrode.

interference. Finally, this electrode is totally encapsulated in PDMS. In order to enhance the attachment between the top and bottom PDMS encapsulation layers, small through-holes are spread as shown in Figure 7(b). A schematic illustration of the cross-sectional view of the electrode is shown in Figure 7(c). The total thickness of the electrode was 100 μm to augment the flexibility and the conformal contact with curved surface.

Fabrication

In Figure 8, the detailed electrode fabrication process is depicted. In order to minimize the damage to the electrode while separating it from the wafer, a sacrificial layer (Ti 100 Å/Au 300 Å) was deposited on a silicon wafer. This sacrificial layer can prevent the damages caused by the usage of physical or chemical treatment during the detachment procedure[35]. A PI (Durimide7505, Fuji-film Electronic Materials, Japan) layer was spin-coated onto the sacrificial metal-deposited wafer at 4000 rpm to yield a thickness of 2-3 μm and the PI layer thus constructed was for the recording and DRL areas (Figure 8(a))[9,36]. The resulting material was soft-baked on a hot plate at 100°C for 3 min, and an aligner (MDA-400S, MIDAS System, Korea) was used to direct UV light onto the PI-layered wafer through a photomask. The wafer was subsequently baked on a hot plate at 60°C for 1 min, and the UV unexposed PI layer was eliminated via incubation in a QZ 3501 (Fuji-film Electronic Materials, Japan) developer solution. After rinsing the wafer with QZ 3512 (Fuji-film Electronic Materials, Japan) solution, titanium (300 Å) and gold (1000 Å) layers were deposited on the developed PI layer wafer to form the recording and DRL layers using an e-beam evaporator. Subsequently,

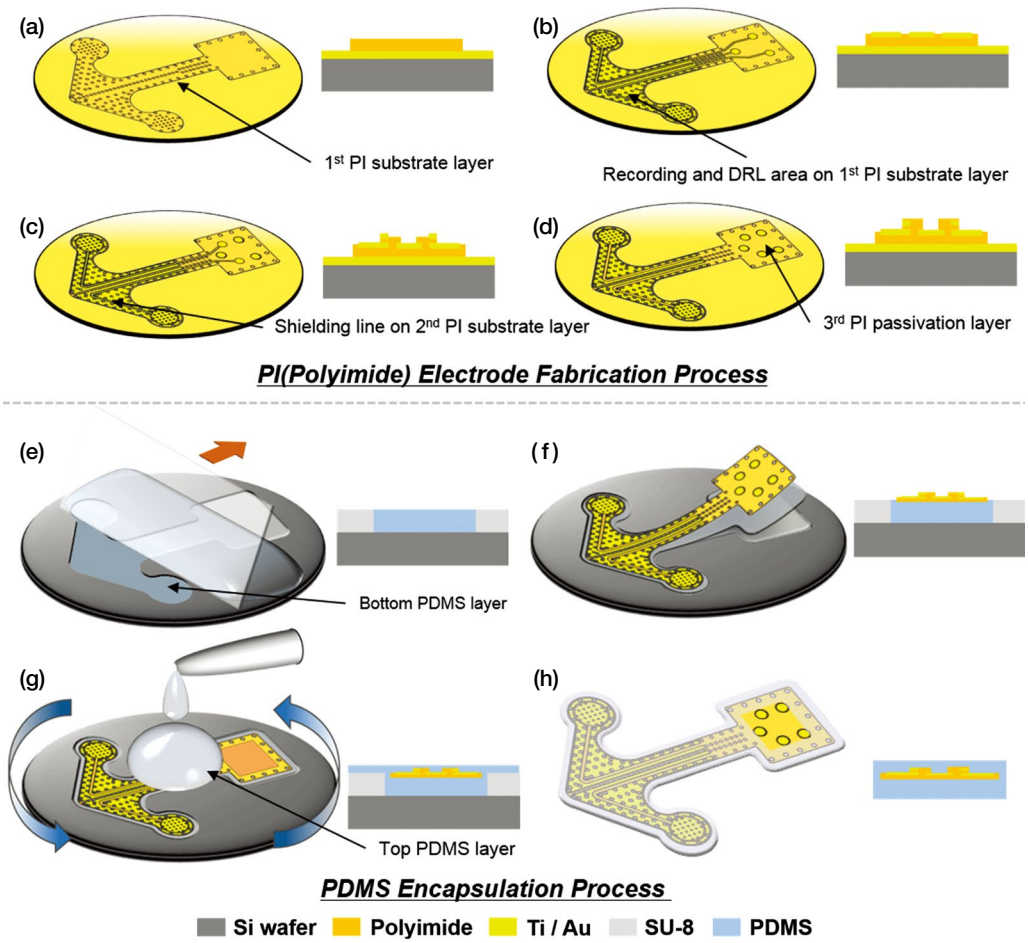

Figure 8. Schematic diagram showing the procedure used to fabricate an electrode. (a) First PI layer, (b) Deposition and patterning of the metal for recording and DRL sites, (c) Second PI layer and patterned shielding line, (d) Passivation PI layer, (e) The PDMS was raked out of the SU-8 mold, (f) PI electrode positioning on the PDMS, (g) A PDMS layer was spin-coated onto the PI electrode and mold, after covering the interconnection area with Kapton® tape, and (h) Detachment of the completed electrode.

AZ GXR-601 solution (16 cp, positive photoresist (PR), AZ Electronic Materials, UK) was spin-coated onto the structure at 3000 rpm for 30 s for the sacrificial layer, which is for a pattern on the deposited metal layer, and baked on hot plate for 1 min at 100°C. After radiating UV light on the PR coated wafer through a metal line patterned photo mask, the layer was developed using the AZ 300 MIF (AZ Electronic Materials, UK) developer. The wafer was incubated in HCl/HNO_3 (3 : 1) and $H_2O/HF/HNO_3$ (50 : 1 : 1) sequentially to remove the unprotected Au and Ti layers. The remaining PR (AZ GXR-601) was removed by washing the wafer in acetone (Figure 8(b)). In order to form the PI layer for the interconnection between the shielding line and metal layer, PI was spin-coated at 4000 rpm for 30 s, and baked at 100°C for 3 min. After forming the pattern and developing the PI layer, a metal layer for the shielding line was deposited and etched away using the aforementioned procedure (Figure 8(c)). Another PI layer was formed to passivate the interconnection line (Figure 8(d)). The wafer was hard-baked on a hot plate for 1 h at 350°C, and subsequently a voltage of 4.0 V was applied on the sacrificial metal layer wafer in the saline solution for the detachment of the electrode from the wafer. A platinum net was also immersed in the saline solution, which behaves as an anode whereas the sacrificial layer on the wafer acts as a cathode. After the completion of PI electrode fabrication, an SU-8 mold was prepared for the PDMS encapsulation of the electrode. A 100 μm thick SU-8 mold in the shape of a slightly enlarged negative electrode pattern was prepared, and PDMS (Sylgard 184 Silicone Elastomer, Dow Corning, USA) was poured into the mold, and raked out with a flat slide glass (Figure 8(e)). After the curing procedure of PDMS, O_2 plasma was directed onto the surface of the PDMS-cured wafer to enhance the conformal contact between the PI electrode and the PDMS layer (Figure 8(f)). The interconnection pad was covered with Kapton® tape before coating another PDMS layer for the encapsulation. Subsequently, PDMS was poured onto the wafer and spin-coated at 2000 rpm for 5 min to achieve a layer of thickness 10-15 μm (Figure 8(g))[37]. After the completion of the curing of the PDMS layer, the PDMS-encapsulated electrode was detached from the SU-8 mold (Figure 8(h)). Further, Kapton® tape was detached from the electrode, and a wire was connected to the pad for connecting an external device.

Active Electrode

The electrode was thoroughly encapsulated by the PDMS layer, which prevented any direct contact between the metal and tissues for recording the ECG signal. Further, a preamplifier was utilized to acquire the ECG signal through the PDMS layer, which has high impedance. This preamplifier must have extremely high input impedance[19,32]. In this study, we used OPA124 (Texas Instruments, US) with an input impedance of 10^{13} Ω and an input capacitance of 1 pF. As shown in Figure 9(a), detailed preamplifier system components are symbolized. First, the resistance and capacitance of the PDMS encapsulation layer are denoted as R_{PDMS} and C_{PDMS}. Further, R_a and C_a represent the resistance and capacitance of preamplifier, respectively. Furthermore, R_{bias}, the bias resistor, allowed bypassing of the accumulated static charges created by the ultra-high input impedance. Further, two parallel metal shielding lines at a distance of 2-3 μm were formed by the PI layer to prevent external noise interference in the in-

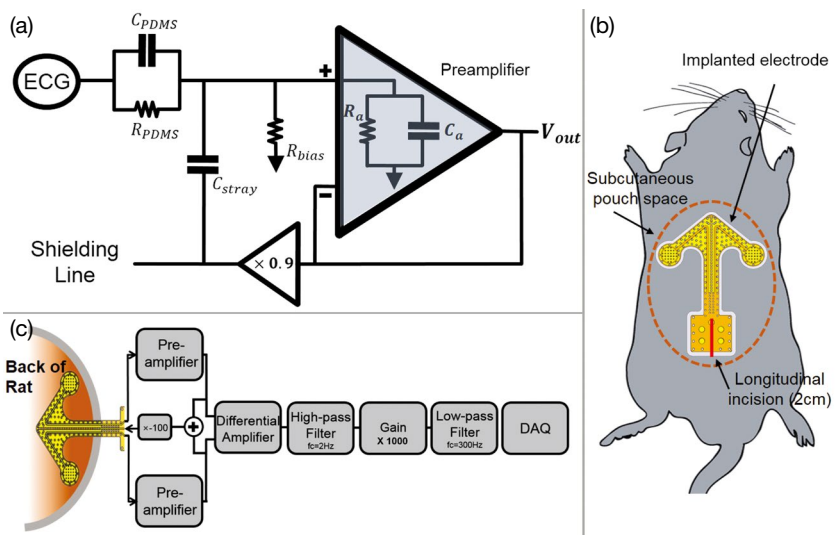

Figure 9. (a) Diagram of preamplifier with active shielding. (b) Schematic illustration of electrode placement and incision on a rat. Subcutaneous pouch was made and electrode was introduced through longitudinal incision as described. (c) Block diagram of acquisition system.

terconnection line. However, these parallel metal lines create a stray capacitance (C_{stray}). The transfer function of preamplifier system can be calculated as follows.

$$G(s)=\frac{V_{out}}{V_{in}}=\frac{R_{bias}(s\cdot R_{PDMS}\cdot C_{PDMS}+1)}{R_{PDMS}+R_{bias}+s\cdot R_{bias}\cdot R_{PDMS}(C_{PDMS}+C_{stray}(1-A_f))} \quad (1)$$

In order to minimize the effect of C_{stray}, ideally, the output voltage of the preamplifier should be applied on the shielding line ($A_f = 1$). However, since this can lead to system oscillations owing to positive feedback, A_f was reduced to 0.9 V/V. We also selected a 50 GΩ resistance as R_{bias}, which is the largest commercially available resistance, to stabilize the signal baseline[29].

Animal Experiment

In this study, all the animal experiments were conducted under the approval of the Korea University Institutional Animal Care & Use Committee. Three male Sprague Dawley (SD) rats, weighing approximately 350-400 g (at 10 weeks), was used for the study. Before implantation, the electrode was sterilized with ethylene oxide (EO) gas. Rats were anesthetized with a mixture of Zoletil (Virbac, 0.1 mL/100 g) and Rompun (Bayer, 0.025 mL/100 g) via intra-peritoneal injection. The epilation was performed on the dorsal area of the rat, which was incised for insertion of the electrode. After the disinfection of the surgical area with an alcohol swab, a longitudinal incision of approximately 2 cm of was made on the dorsal area of the rat as shown in Figure 9(b). After the incision, an inner subcutaneous pouch was made with blunt surgical scissors. The size of the pouch should be just large enough to accommodate the electrode, so that the electrode does not to move freely in the subcutaneous area. The electrode was positioned in the subcutaneous area and adjusted. The incision was closed with wound clips and wires were pulled out between the wound clips. The surgical area was disinfected every day.

Impedance Measurements and Equivalent Circuit Analysis

The impedance electrical characteristics of electrode were measured using electrochemical impedance spectroscopy (EIS) (Series G300, Gamry instrument, USA). By sweeping the frequency range of the electrode from 0.1 to 1 kHz in a PBS solution of pH 7.4, we could acquire the impedance information over a similar frequency range of ECG of the rat. Five electrodes were immersed in the PBS solution to observe the impedance variation. The impedance of the electrode was measured on days 0, 3, 7, 14, 21, and 28 in the PBS solution. The immersed electrodes and the PBS solution were sealed with Parafilm® to prevent evaporation and kept in a convective oven at 36°C. We assumed that the impedance of PDMS is parallelized with a resistor (R_{PDMS}) and a capacitor (C_{PDMS}) as shown in Figure 9(a). The equivalent circuit of R_{PDMS} and C_{PDMS} were simulated by applying the curve-fitting method using MATLAB, and subsequently the PBS uptake effects on the impedance of PDMS was simulated, too.

Noise Power Density Spectrum

The power spectrum density (PSD) was calculated to acquire the noise characteristics of the electrode. A platinum mesh and electrode were immersed in the PBS solution (pH 7.4). The signal was measured while the platinum mesh was connected to ground. The measurement was repeated after 4 weeks.

Leakage Current

The electrode was placed on a copper plate to measure the current leaking through the electrode. A 1 kΩ resistor and the cathode of a SourceMeter® (Model 2400, KEITHLEY, USA) were connected to the electrode in parallel, and the copper plate was connected to the anode of the SourceMeter®. The current applied to the electrode and resistor was increased from 0 to 10 mA. Subsequently, the current that passes through the electrode and the copper plate was measured. A direct contact electrode, PDMS-encapsulated electrode, and PDMS-encapsulated electrode kept in PBS for 100 days were evaluated in the leakage test.

In vivo Biocompatibility Test

The biocompatibility test was performed by implanting an electrode on the back of the SD rat and kept for a month. The tissue was histologically analyzed via hematoxylin and eosin staining (H&E staining) after 4 weeks, and the status of the electrode was inspected visually.

ECG Measurements

The electrode can be functionally split into three different parts: two recording sites, DRL area, and shielding line. Figure 9(c) shows a schematic illustration of the signal acquiring system. The signals from both recording sites were subtracted for the acquisition of the ECG signal. Further, INA114 (Burr-Brown), a differential amplifier, was used for the subtraction of signals. The signal was filtered through a second-order high ($f_c = 2$ Hz) and low ($f_c = 300$ Hz) pass filter to eliminate

fluctuation and to prevent aliasing. The signal was amplified with a gain of 1000 V/V and digitized at 10 kHz using an analog-to-digital converter (NI USB-6225, National Instruments, USA). While the ECG signals from a subject are being measured, the common voltage of the subject should be minimized to prevent ECG from deteriorating. The DRL method was used to reduce the common noise[32]. The two signals from the two recording sites were summed up, and a negative gain of 100 V/V was applied on the DRL site. Since the signal detection is made through the PDMS layer, which has high impedance, the size of the contact area is critical for the capacitive characteristics[33]. Three different sizes of electrodes (small (*r*: 1.8 mm), medium (*r*: 2.8 mm), and large (*r*: 3.8 mm)) were fabricated to test the effect of size of the recording area on the signal. These three electrodes were implanted into three different rats, and the signal was acquired on days 0, 3, and 7 after implantation to observe the signal changes.

Acknowledgements This work is dedicated to the late Professor Sang-Hoon Lee, one of the great pioneers of biomedical engineering, who passed away while attending the Gordon Research Conference 2016 in Hong Kong. This research was supported by a grant from the Korea Health Technology R&D Project through the Korea Health Industry Development Institute (KHIDI), funded by the Ministry of Health & Welfare, Republic of Korea (grant no.: HI14C0522), 2013 Research Grant form Kangwon National University (No. C1010260-01-01), the Basic Science Research Program through the National Research Foundation of Korea (NRF) funded by the Ministry of Education (2017R1D1A1A02019351, 2014R1A1A2056873) and the Korea Government (MSIP) (NRF-2016R1A5A1012966).

References

1. Arzbaecher, R., Hampton, D.R., Burke, M.C. & Garrett, M.C. Subcutaneous electrocardiogram monitors and their field of view. *J. Electrocardiol.* **43**, 601-605 (2010).
2. Iglesias, J.F., Graf, D., Pascale, P. & Pruvot, E. The implantable loop recorder: a critical review. *Kardiovask. Med.* **12**, 85-93 (2009).
3. Manolis, A.S., Linzer, M., Salem, D. & Estes, N.M. Syncope: current diagnostic evaluation and management. *Ann. Intern. Med.* **112**, 850-863 (1990).
4. Nei, M. *et al.* EEG and ECG in sudden unexplained death in epilepsy. *Epilepsia* **45**, 338-345 (2004).
5. Jeong, G.S. *et al.* Solderable and electroplatable flexible electronic circuit on a porous stretchable elastomer. *Nat. Commun.* **3**, 977 (2012).
6. Jeong, J.W. *et al.* Capacitive Epidermal Electronics for Electrically Safe, Long-Term Electrophysiological Measurements. *Adv. Healthc. Mater.* **3**, 642-648 (2014).
7. Kim, D.-H. *et al.* Epidermal electronics. *Science* **333**, 838-843 (2011).
8. Lee, J.H. *et al.* Shear induced CNT/PDMS conducting thin film for electrode cardiogram (ECG) electrode. *BioChip J.* **6**, 91-98 (2012).
9. Baek, D.-H. *et al.* A dry release of polyimide electrodes using Kapton film and application to EEG signal measurements. *Microsyst. Technol.* **17**, 7-14 (2011).
10. Chou, N., Yoo, S. & Kim, S. A largely deformable surface type neural electrode array based on PDMS. *IEEE Trans. Neural Syst. Rehabil. Eng.* **21**, 544-553 (2013).
11. Chui, R.W., Derakhchan, K. & Vargas, H.M. Comprehensive analysis of cardiac arrhythmias in telemetered cynomolgus monkeys over a 6 month period. *J. Pharmacol. Toxicol. Methods* **66**, 84-91 (2012).
12. Cools, F. *et al.* ECG arrhythmias in non-implanted vs. telemetry-implanted dogs: Need for screening before and sufficient recovery time after implantation. *J. Pharmacol. Toxicol. Methods* **64**, 60-67 (2011).
13. Moxon, K.A. *et al.* Nanostructured surface modification of ceramic-based microelectrodes to enhance biocompatibility for a direct brain-machine interface. *IEEE Trans. Biomed. Eng.* **51**, 881-889 (2004).
14. Vince, V., Thil, M.-A., Veraart, C., Colin, I. & Delbeke, J. Biocompatibility of platinum-metallized silicone rubber: in vivo and in vitro evaluation. *J. Biomater. Sci. Polym. Ed.* **15**, 173-188 (2004).
15. Hassler, C., Boretius, T. & Stieglitz, T. Polymers for neural implants. *J. Polym. Sci. Part B Polym. Phys.* **49**, 18-33 (2011).
16. Ordonez, J.S., Boehler, C., Schuettler, M. & Stieglitz, T. Improved polyimide thin-film electrodes for neural implants. in *2012 Annual International Conference of the IEEE EMBS* 5134-5137 (IEEE, 2012).
17. Viventi, J. *et al.* Flexible, foldable, actively multiplexed, high-density electrode array for mapping brain activity in vivo. *Nat. Neurosci.* **14**, 1599-1605 (2011).
18. Torres, F., Das Graças, M., Melo, M. & Tosti, A. Management of contact dermatitis due to nickel allergy: an update. *Clin. Cosmet. Investig. Dermato.* **2**, 39 (2009).
19. Xu, S. *et al.* Stretchable batteries with self-similar serpentine interconnects and integrated wireless recharging systems. *Nat. Commun.* **4**, 1543 (2013).
20. Kim, S.H., Moon, J.-H., Kim, J.H., Jeong, S.M. & Lee, S.-H. Flexible, stretchable and implantable PDMS encapsulated cable for implantable medical device. *Biomed. Eng. Lett.* **1**, 199-203 (2011).
21. Nair, B. Final report on the safety assessment of stearoxy dimethicone, dimethicone, methicone, amino bispropyl dimethicone, aminopropyl dimethicone, amodimethicone, amodimethicone hydroxystearate, behenoxy dimethicone, C24-28 alkyl methicone, C30-45 alkyl methicone, C30-45 alkyl dimethicone, cetearyl methicone, cetyl dimethicone, dimethoxysilyl ethylenediaminopropyl dimethicone, hexyl methicone, hydroxypropyldimethicone, stearamidopropyl di-

methicone, stearyl dimethicone, stearyl methicone, and vinyldimethicone. *Int. J. Toxicol.* **22**, 11-35 (2002).
22. Gao, A.X., Tian, Y.L., Shi, Z.Z. & Yu, L. A Cost-effective Microdevice Bridges Microfluidic and Conventional in vitro Scratch/Wound-healing Assay for Personalized Therapy Validation. *BioChip J.* **10**, 56-64 (2016).
23. Belanger, M.C. & Marois, Y. Hemocompatibility, biocompatibility, inflammatory and in vivo studies of primary reference materials low-density polyethylene and polydimethylsiloxane: a review. *J. Biomed. Mater. Res.* **58**, 467-77 (2001).
24. Lee, K.K. *et al.* Polyimide-based intracortical neural implant with improved structural stiffness. *J. Micromech. Microeng.* **14**, 32-37 (2004).
25. Moon, J.H. *et al.* Wearable polyimide-PDMS electrodes for intrabody communication. *J. Micromech. Microeng.* 20 (2010).
26. Cheung, K.C., Renaud, P., Tanila, H. & Djupsund, K. Flexible polyimide microelectrode array for in vivo recordings and current source density analysis. *Biosens. Bioelectron.* **22**, 1783-1790 (2007).
27. Webster, J. in *Medical instrumentation: application and design* (John Wiley & Sons, 2009).
28. Winter, B.B. & Webster, J.G. Reduction of interference due to common mode voltage in biopotential amplifiers. *IEEE Trans. Biomed. Eng.* **30**, 58-62 (1983).
29. Lee, S.M. *et al.* A capacitive, biocompatible and adhesive electrode for long-term and cap-free monitoring of EEG signals. *J. Neural. Eng.* **10**, 036006-036014 (2013).
30. Delivopoulos, E., Chew, D.J., Minev, I.R., Fawcett, J.W. & Lacour, S.P. Concurrent recordings of bladder afferents from multiple nerves using a microfabricated PDMS microchannel electrode array. *Lab Chip* **12**, 2540-2551 (2012).
31. Li, T., Huang, Z.Y., Suo, Z., Lacour, S.P. & Wagner, S. Stretchability of thin metal films on elastomer substrates. *Appl. Phys. Lett.* **85**, 3435-3437 (2004).
32. Lee, S.M., Sim, K.S., Kim, K.K., Lim, Y.G. & Park, K.S. Thin and flexible active electrodes with shield for capacitive electrocardiogram measurement. *Med. Bio. Eng. Comput.* **48**, 447-457 (2010).
33. Ueno, A. *et al.* Capacitive sensing of electrocardiographic potential through cloth from the dorsal surface of the body in a supine position: a preliminary study. *IEEE Trans. Biomed. Eng.* **54**, 759-766 (2007).
34. Fernandes, M., Lee, K., Ram, R., Correia, J. & Mendes, P. Flexible PDMS-based dry electrodes for electro-optic acquisition of ECG signals in wearable devices. in *2010 Annual International Conference of the IEEE Eng Med Biol Soc.* 3503-3506 (IEEE, 2010).
35. Metz, S., Bertsch, A. & Renaud, P. Partial release and detachment of microfabricated metal and polymer structures by anodic metal dissolution. *J. Microelectromech. Syst.* **14**, 383-391 (2005).
36. Sun, Y. *et al.* Assessment of the biocompatibility of photosensitive polyimide for implantable medical device use. *J. Biomed. Mater. Res. A* **90**, 648-655 (2009).
37. Koschwanez, J.H., Carlson, R.H. & Meldrum, D.R. Thin PDMS films using long spin times or tert-butyl alcohol as a solvent. *PLoS ONE* **4**, e4572 (2009).